

Photophysical Probes of a Protein/Semiconductor Electrode Interface

Liang-Hong Guo, Shaul Mukamel, and George McLendon*

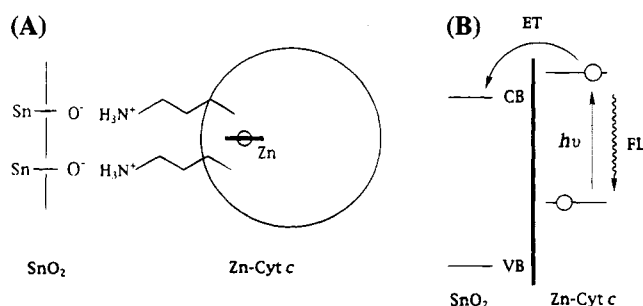
Department of Chemistry and
Center for Photoinduced Charge Transfer
University of Rochester
Rochester, New York 14627-0216

Received September 26, 1994

Immobilization of redox molecules on solid electrodes offers a way of investigating the electron transfer of a donor/acceptor interface without the presence of diffusion processes.¹ Such interactions also have important implications for analytical and clinical biochemistry. Direct electrochemistry of proteins and enzymes is therefore an active research field.² One example of direct protein electrochemistry relevant to this work is cytochrome *c* (Cyt *c*) adsorbed on a tin oxide (SnO₂) surface.^{1b} This protein is rich in lysine amino acid residues and thus carries positive charges at neutral pH. It has been found that the native protein, Fe-Cyt *c*, adsorbs strongly on SnO₂, presumably through the electrostatic interaction with the deprotonated hydroxyl groups on SnO₂ surface (Scheme 1A). The electron transfer rate constant between the two at zero free energy has been measured by cyclic voltammetry and is found to be relatively slow (3–8 s⁻¹). In terms of modern theoretical understanding of electron transfer,³ the parameters (electronic coupling, *V*, and reorganization energy, λ) which govern this rate remain uncharacterized. We report here a novel approach to obtain such parameters by combining thermal and photochemical interfacial electron transfer measurements within the context of a novel theoretical formalism. We used time-resolved fluorescence spectroscopy to measure the interfacial electron transfer rate constant from zinc-substituted cyt *c* (Zn-Cyt *c*) to SnO₂ and estimated electronic coupling between the protein and semiconductor and the reaction reorganization energy. The lowest photoexcited state of Zn-Cyt *c* has a much higher energy level⁴ than the conduction band edge⁵ of SnO₂ (Scheme 1B). Electron injection to SnO₂ (route a in Scheme 1B) is therefore a thermodynamically favorable process that competes with fluorescent decay emission (route b).

Zn-Cyt *c* was prepared⁶ and adsorbed^{1b,7} onto a fluorine-doped SnO₂ substrate according to the published procedures. The adsorption was confirmed by the UV–vis spectrum of Zn-Cyt *c* and cyclic voltammogram of the native Fe-Cyt *c*. Integration of either the anodic or the cathodic wave in the voltammogram yielded a surface coverage of 5–10 pmol/cm², which is substantially less than the calculated full monolayer coverage of about 20 pmol/cm², by assuming the diameter of

Chart 1. (A) Illustration of the Mode of Electrostatic Interaction between the Lysine Residues on Cyt *c* (–NH₃⁺) and the Hydroxyl Groups on SnO₂ Surface (–SN–O⁻)^a and (B) Diagram of the Energy Levels in Cyt *c* and SnO₂ and Possible Routes of Deexcitation of the Excited Electrons^b



^a The schematic is for illustrative purpose only and is not drawn to scale. For example, Cyt *c* is roughly spherical in shape and has a diameter of 30 Å.^b (a) interfacial electron injection (ET), and (b) fluorescence (FL) emission.

Cyt *c* as 30 Å. Protein-adsorbed SnO₂ samples were removed from solution and used in the fluorescence experiments. When excited with 582 nm light, Zn-Cyt *c* gave a broad emission spectrum with a maximum at 640 nm, where SnO₂ alone did not emit. Time-resolved fluorescence emissions were collected by the single photon counting technique and are shown in Figure 1. The emission curves of Zn-Cyt *c* both on SnO₂ and on glass (on which there is no interfacial ET) can be fitted reasonably well with double-exponential decay. The lifetime of the major component is in the range of 10⁻⁹ s and is shorter on SnO₂ than on glass by 30%, resulting in an average radiationless rate constant of 2 × 10⁸ s⁻¹. Energy transfer between protein molecules is unlikely since the surface coverage is submonolayer. We also ruled out the possibility of energy transfer between the protein and SnO₂ due to the fact that this semiconductor does not absorb light at the excitation wavelength. Therefore, apart from fluorescence, electron injection from the excited Zn-Cyt *c* to SnO₂ seems to be the only route for de-excitation. Photoinduced interfacial electron transfer is confirmed by the observation of anodic photocurrents of Zn-Cyt *c*/SnO₂ sample immersed in an electrochemical cell (Figure 2a). The photocurrent excitation spectrum (Figure 2b) corresponds to the UV–vis spectrum of Zn-Cyt *c* in aqueous solution. Bare SnO₂ did not show such behavior.

With these data available, information on two key parameters can be obtained, as follows. First, since the high density of acceptor states ensures an optimal Franck–Condon factor, the electronic coupling can be assessed directly from the electron transfer rate constant. The observed rate is relatively slow in comparison with (similar) photoexcited dye molecules directly adsorbed to a semiconductor surface, which exhibited subpicosecond electron injection.⁸ Thus the rate of electron injection from bound Cyt *c* is nominally 10⁴ slower than that for directly adsorbed dyes. This suggests an interfacial interaction in which the reactive zinc porphyrin is relatively sequestered from the semiconductor surface by the intervening protein matrix. If one uses the broadest assumption of an exponential decay of rate with distance³, $k \propto \exp(-\beta R)$, with $\beta \approx 1.4 \text{ \AA}^{-1}$, the porphyrin

(7) The following is a brief description of the procedure: SnO₂ was sonicated sequentially in alconox, ethanol, and water and rinsed with water after each solution. It was then equilibrated overnight with a phosphate buffer (2.2 mM, pH 7.0). Finally, the substrate was immersed for 20 min in a dilute solution of Cyt *c* dissolved in the phosphate buffer. The SnO₂ electrode was removed from Cyt *c* solution, dipped in buffer to remove unadsorbed Cyt *c*. Large droplets were removed under an argon stream. This procedure retains a layer of relatively tightly bound solvent at the cytochrome/electrode interface.

(8) Lanzafame, J. M.; Miller, R. J. D.; Muentzer, A. A.; Parkinson, B. A. *J. Phys. Chem.* 1992, 96, 2820.

(1) (a) Li, T. T.; Weaver, M. J. *J. Am. Chem. Soc.* 1984, 106, 6107. (b) Willit, J. L.; Bowden, E. F. *J. Electroanal. Chem.* 1987, 221, 265. (c) Chidsey, C. E. D. *Science* 1991, 251, 919. (d) Tarlov, M. J.; Bowden, E. F. *J. Am. Chem. Soc.* 1991, 113, 1847. (e) Finklea, H. O.; Hanshew, D. D. *J. Am. Chem. Soc.* 1992, 114, 3173. (f) Facci, J. S. In *Techniques of Chemistry*; Murray, R. W., Ed.; Wiley-Interscience: New York, 1993; Vol. XXII, Chapter 3 and references therein.

(2) (a) Bowden, E. F.; Hawkring, F. M.; Blount, H. N. In *Comprehensive Treatise of Electrochemistry*; Srinivasan, S., Chizmadzhev, Y. A., Bockris, J. O'M., Conway, B. E., Yeager, E., Eds.; Plenum Press: New York, 1985; Vol. 10, p 297. (b) Armstrong, F. A.; Hill, H. A. O.; Walton, N. J. *Acc. Chem. Res.* 1988, 21, 407. (c) Guo, L.-H.; Hill, H. A. O. In *Advances in Inorganic Chemistry*; Sykes, A. G., Ed.; Academic Press: San Diego, CA, 1991; Vol. 36, p 341. (d) Heller, A. *J. Phys. Chem.* 1992, 96, 3579. (e) Armstrong, F. A. In *Advances in Inorganic Chemistry*; Sykes, A. G., Ed.; Academic Press: San Diego, CA, 1992; Vol. 38, p 117.

(3) Marcus, R. A.; Sutin, N. *Biochim. Biophys. Acta* 1985, 811, 265.

(4) Magner, E.; McLendon, G. *J. Phys. Chem.* 1989, 93, 7130.

(5) Fox, M. A. In *Advances in Electron Transfer Chemistry*; Mariano, P. S., Ed.; JAI Press Inc.: London, 1991; Vol. 1, p 1.

(6) (a) Vandervooi, J. M.; Adar, F.; Erecinska, M. *Eur. J. Biochem.* 1976, 64, 381. (b) McLendon, G.; Miller, J. R. *J. Am. Chem. Soc.* 1985, 107, 7811.

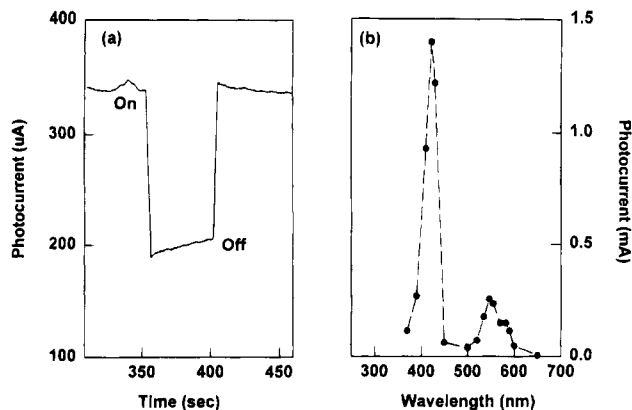


Figure 1. Time-resolved fluorescence spectra of Zn-Cyt *c* on glass and SnO₂ collected by time-correlated single photon counting (SPC) method. The dotted line is for the experimental data, and the dashed line is the fitting curve composed of double exponential decay. (a) Zn-Cyt *c* on glass, $\tau_1 = 3.4 \times 10^{-10}$ s, $\tau_2 = 1.5 \times 10^{-9}$ s, $\chi^2 = 1.16$, and the average values from five measurements are $\tau_1 = 3.4 \times 10^{-10}$, $\tau_2 = 1.4 \times 10^{-9}$ s (standard deviation, 6%). (b) Zn-Cyt *c* on SnO₂, $\tau_1 = 2.6 \times 10^{-10}$ s, $\tau_2 = 1.0 \times 10^{-9}$ s, $\chi^2 = 1.03$, and the averages are $\tau_1 = 3.0 \times 10^{-10}$ s, $\tau_2 = 1.1 \times 10^{-9}$ s (standard deviation, 8%). SPC was performed with an excitation system made up of a mode-locked, frequency-doubled Nd:YAG laser (Quantronix Model 416) synchronously pumping a cavity-dumped dye laser (Coherent, Model 703D) circulating dye 801. The Nd:YAG laser produces a series of pulses of 5 ps in duration at a repetition rate of 38 MHz. The time resolution of the system is 9.876 ps/channel.

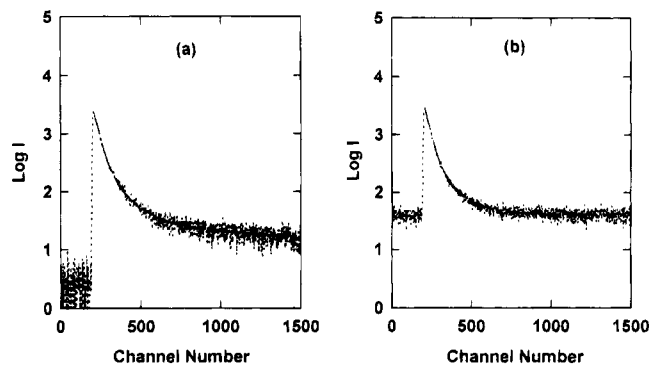


Figure 2. (a) Time-based photocurrent of Zn-Cyt *c* adsorbed on SnO₂ with 582 nm excitation. The light was switched on and off as marked. Photocurrents were measured with a BAS 100A electrochemical analyzer and a PTI A1010 monochromator. The samples were immersed in an electrochemical cell containing 2 mM K₄Fe(CN)₆ in a phosphate buffer (2.2 mM, pH 7.0). The potential of the SnO₂ electrode was held at 0 V vs Ag/AgCl. (b) Plot of the photocurrent as a function of the excitation wavelength.

group would be about 6 Å away from the SnO surface. This distance corresponds reasonably to the geometry expected for binding of the protein to the solid surface through extended lysine side chains, as suggested by the schematic representation in Scheme 1A.

Second, the reorganization energy can also be estimated. The electronic coupling matrix element derived from the result gives a value in terms of energy/state, rather than the more familiar integral over all states, which is valid for thermal electron transfer occurring at the Fermi level. In the limit of sparse electronic states, we can use the Marcus two-state expression. The continuum necessary for obtaining a rate is then derived from the nuclear degrees of freedom (the reorganization energy). We then have³ for $\Delta G^\circ = 0$,

$$K_2 = \frac{1}{h} \sqrt{\frac{\pi}{\lambda kT}} |V|^2 \exp\left(-\frac{\lambda}{4kT}\right) \quad (1)$$

When the system is coupled to an electronic continuum and the nuclear degrees of freedom are neglected, we start with the

Fermi golden rule:

$$K_1 = \frac{2\pi}{h} |V|^2 \rho \quad (2)$$

In eqs 1 and 2, K_1 and K_2 are the interfacial electron transfer rate constants, V and V' the electronic coupling, and ρ the density of final electronic states. The following points should be made: (a) V' is different from V . V' is the coupling per state, whereas V is the total integrated coupling. We can write $N|V|^2 = |V'|^2$, where N is the effective number of strongly coupled electronic states. (b) K_1 is not generally proportional to the density of states. Equation 2 is somewhat misleading. In practice, when ρ is large, then $|V|^2 \propto 1/\rho$, so that we reach a thermodynamic limit where the rate does not depend on the density of states.

We can estimate N by recognizing that the energy uncertainty (line width) associated with the initial state due to the Heisenberg principle is $\Delta E = hK_1$. The number of states in this energy range is $N = \Delta E \rho$. Putting all of these together, we get

$$K_1 = \frac{2\pi |V|^2}{h h K_1}$$

so that

$$K_1^2 = 2\pi |V|^2/h^2 \quad (3)$$

Dividing eqs 3 and 1, we finally obtain

$$\frac{h}{2\sqrt{\pi} kT K_2} K_1^2 = \sqrt{x} \exp(x/4) \quad (4)$$

with $x = \lambda/kT$.

Measurement of K_1 and K_2 can thus lead to an estimate of λ . Using the values of $K_1 = 2 \times 10^8$ s⁻¹ from the Zn-Cyt *c*/SnO₂ system and $K_2 = 5$ s⁻¹ from the Fe-Cyt *c*/SnO₂ system,^{1b} we have⁹

$$\sqrt{x} \exp(x/4) = 54$$

solving for x we obtain

$$\lambda = 0.28 \text{ eV}$$

The reorganization energy of Cyt *c* has been measured or estimated before by many research groups¹⁰ using different physical methods, with values ranging from 0.14 to 1.2 eV. Our value of 0.28 eV falls within the range.¹¹

In summary, when photophysical luminescence techniques can be coupled with photoelectrochemical techniques, they together can provide unique insights into the nature of the protein/electrode interaction in direct protein electrochemistry. This approach, when applicable, can also provide a direct estimate of the fundamental parameters governing interfacial electron transfer, i.e., the electronic coupling and the reorganization energy.

Acknowledgment. We are grateful to Dr. E. F. Bowden of North Carolina State University for supplying the tin oxide samples and both Drs. Bowden and R. J. D. Miller for helpful discussions. This work is supported by a grant from the NSF Center for Photoinduced Charge Transfer (CHE-9120001).

JA943168R

(9) The estimated λ has some uncertainty due to the variation of the fluorescence lifetimes measured by SPC. However, the uncertainty is very small. For example, variation of $\pm 10\%$ in lifetimes would result in an uncertainty of only ± 0.01 eV for λ .

(10) (a) Bowler, B. E.; Meade, T. J.; Mayo, S. L.; Richards, J. H.; Gray, H. B. *J. Am. Chem. Soc.* **1989**, *111*, 8757. (b) Dixon, D. W.; Hong, X.; Woehler, S. E.; Mauk, A. G.; Sista, B. P. *J. Am. Chem. Soc.* **1990**, *112*, 1082. (c) Cho, K. C.; Chu, W. F.; Choy, C. L.; Che, C. M. *Biochim. Biophys. Acta* **1989**, *973*, 53. (d) Dickerson, R. E.; Takano, T.; Eisenberg, D.; Kallai, O. B.; Samson, L.; Cooper, A.; Margoliash, E. *J. Biol. Chem.* **1971**, *246*, 1511.

(11) Note that this analysis provides the value of λ for Fe-Cyt *c* only. It need not assume an equivalent value of λ for Zn-Cyt *c*, since the value of λ for Zn does not control the photochemical rate. This rate constant depends on $|V|^2$, which depends only on the structure of the Cyt *c*/SnO₂ interface and on the electronic density of states of the semiconductor.